A robust adaptive controller for underactuated ASVs in loose path-following with an added error and a new control handpoint

Cao Duc Sang*, Le Tran Thang, Nguyen Trong Khuyen

Institute of Automation, Academy of Military Science and Technology, 89B Ly Nam De, Hoan Kiem, Hanoi, Vietnam.

*Corresponding author: sangdctech@gmail.com

Received 23 May 2025; Revised 16 Jul. 2025; Accepted 20 Sep. 2025; Published 2 Oct. 2025.

DOI: https://doi.org/10.54939/1859-1043.j.mst.106.2025.18-27

ABSTRACT

Controlling an ASV to follow a desired trajectory poses a significant challenge due to the unstable structure of its operating environment, which is often affected by disturbances such as wind, ocean waves, and currents. Furthermore, the ASV's dynamic model is typically highly nonlinear and contains many uncertainties. In this work, we develop an adaptive controller for an underactuated ASV to address the path-following problem under uncertain disturbances. To deal with the underactuation, a small error is added to the tracking error, and a new control hand-point technique is applied. The guidance and force adaptive control laws are designed, and their stability is proven using Lyapunov theory. In addition to the theory, Simulations in the MATLAB-Simulink environment are conducted and compared with other methods. Simulation results demonstrate the robustness of the proposed controller under unknown disturbances.

Keywords: Underactuated ASVs; Cross tracking error; Control handpoint; Path-following.

1. INTRODUCTION

For Autonomous Surface Vehicles (ASVs), the path-following problem is often considered complex and challenging. The main reason is the unstable nature of the water environment, which is constantly affected by unpredictable disturbances such as waves, wind, and ocean currents. Additionally, the dynamic model of ASVs is highly nonlinear and underactuated. These factors make a significantly impact on the performance and reliability of a designed controller.

In this problem, a guidance algorithm is typically combined with a force controller. The Line of Sight (LOS) method provides a guidance law for determining the heading angle of the ASV [1, 2]. In this approach, the ASV is directed toward a point located at a predefined look-ahead distance. The force controller is then designed to steer the ASV toward the reference heading generated by the guidance law. Once the ASV reaches this reference angle, the guidance law ensures that the position error between the vehicle and the desired point on the trajectory gradually converges to zero. The LOS method offers advantages, including ease of implementation, reliance on simple geometric principles, straightforward programming, and ease of debugging. The use of a lookahead distance helps to reduce abrupt changes in heading. However, the performance of the LOS method heavily depends on the lookahead distance. If the lookahead distance is too short, the system may become unstable, prone to oscillation and overshoot. Conversely, if the lookahead distance is too large, the system responds slowly. The LOS guidance law can be challenging to apply for precise tracking, particularly in highly disturbed environments.

Other studies employ the Pure Pursuit (PP) [3] or the Vector Field (VF) [4] guidance law. The PP method is commonly used in pursuit missions due to its simplicity and ease of implementation. However, it suffers from poor tracking accuracy and stability. The VF method generates a vector field around the desired trajectory. By controlling the ASV to align its heading with these vectors, the vehicle eventually converges to the desired path. This method is widely used in path-following problems for UAVs. However, its tracking performance heavily depends on the accuracy of the dynamic model, which is challenging to achieve for marine vehicles subject to various uncertain disturbances.

At the dynamic level, the design of a force controller for underactuated ASVs is quite challenging. For the force controller, one of the most commonly used methods is the PID controller [5]. The main advantage of this method is its simplicity in design; however, it is typically sensitive to noise and generally performs well only for linear systems. For nonlinear systems, the Sliding Mode Control (SMC) method is widely used, including in autonomous surface vehicles (ASVs) [6]. The SMC technique can handle model uncertainties and disturbances effectively. However, it often causes chattering in the control input and state variables. Another method that is frequently used and quite effective for nonlinear systems is the backstepping technique [7]. The backstepping controller is recursively constructed by selecting appropriate Lyapunov functions. In [8, 9], the author uses the Model Predictive Control (MPC) technique for the force controller. The advantage of MPC is its ability to optimize control parameters while satisfying input and output constraints, but the stability of the system under MPC is not guaranteed, and it requires a large computational resource. The control performance also depends heavily on the accuracy of the model used. While [8] requires the ASV to be fully actuated, [9] suggests that the ASV model is linear. In [10], the authors incorporated a slight offset from the intended path, defining a bounded region that the vehicle is expected to follow.

In this study, we design a guidance law for the path-following problem based on adding a small error to the discrepancy between the ASV and desired positions. A new control hand-point technique and a similar technique in [10] are applied to deal with the underactuation of the ASV. At the dynamic level, an adaptive force controller with a time-varying adaptive gain is presented to drive the ASV along the desired path in an environment with unknown time-varying disturbances. In addition, uniform asymptotic stability of the complete system is investigated and simulated. The simulation results on Matlab-Simulink for the path-following problem with an underactuated ASV demonstrate the robustness and effectiveness of the proposed controller.

2. METHODOLOGY

2.1. Underactuated ASV model with a new control handpoint

According to [13], the dynamic model of an underactuated ASV is given as:

$$\begin{bmatrix} m_{11} & 0 & 0 \\ 0 & m_{22} & m_{23} \\ 0 & m_{32} & m_{33} \end{bmatrix}\begin{bmatrix} \dot{u} \\ \dot{v} \\ \dot{r} \end{bmatrix} + \begin{bmatrix} 0 & 0 & -c_2 v - c_3 r \\ 0 & 0 & c_1 u \\ c_2 v + c_3 r & -c_1 u & 0 \end{bmatrix}\begin{bmatrix} u \\ v \\ r \end{bmatrix} + \begin{bmatrix} d_{11} & 0 & 0 \\ 0 & d_{22} & d_{23} \\ 0 & d_{32} & d_{33} \end{bmatrix}\begin{bmatrix} u \\ v \\ r \end{bmatrix} = \begin{bmatrix} F \\ 0 \\ T \end{bmatrix} + \begin{bmatrix} \mathrm{w}_1 \\ \mathrm{w}_2 \\ \mathrm{w}_3 \end{bmatrix} \quad (1)$$

Where: $\boldsymbol{M} = \begin{bmatrix} m_{11} & 0 & 0 \\ 0 & m_{22} & m_{23} \\ 0 & m_{32} & m_{33} \end{bmatrix}$, $\boldsymbol{C} = \begin{bmatrix} 0 & 0 & -c_2 v - c_3 r \\ 0 & 0 & c_1 u \\ c_2 v + c_3 r & -c_1 u & 0 \end{bmatrix}$, $\boldsymbol{D} = \begin{bmatrix} d_{11} & 0 & 0 \\ 0 & d_{22} & d_{23} \\ 0 & d_{32} & d_{33} \end{bmatrix}$ are the inertia matrix, the Coriolis and centripetal matrix, and the damping matrix, respectively; $\boldsymbol{\upsilon} = \begin{bmatrix} u & v & r \end{bmatrix}^T$ is the ASV velocity in body frame; F, T are the surge force and yaw moment generated by a propeller and a steering rudder, respectively; $\boldsymbol{w} = \begin{bmatrix} w_1 & w_2 & w_3 \end{bmatrix}^T$ represents unknown time-varying disturbances.

The model (1) can be expanded as follows:

$$\begin{cases} \dot{u} = f_u(u,v,r) + b_u F + \delta_u \\ \dot{v} = f_v(u,v,r) + b_v T + \delta_v \\ \dot{r} = f_r(u,v,r) + b_r F + \delta_r \end{cases} \quad (2)$$

Where: $b_u = \dfrac{1}{m_{11}}$; $b_v = \dfrac{-m_{23}}{m_{22}m_{33} - m_{23}m_{32}}$; $b_r = \dfrac{m_{22}}{m_{22}m_{33} - m_{23}m_{32}}$; $f_u = \dfrac{c_2 vr + c_3 r^2 - d_{11}u}{m_{11}}$;

$$f_v = \frac{m_{23}(c_1 - c_2)uv + (m_{33}c_1 - m_{23}c_3)ur + (m_{33}d_{22} - m_{23}d_{32})v + (m_{33}d_{23} - m_{23}d_{33})r}{-m_{22}m_{33} + m_{23}m_{32}};$$

$$f_r = \frac{m_{22}(c_1 - c_2)uv + (m_{22}c_3 - m_{32}c_1)ur + (m_{33}d_{22} - m_{23}d_{22})v + (m_{22}d_{23} - m_{32}d_{23})r}{-m_{22}m_{33} + m_{23}m_{32}};$$

$$\delta_u = \frac{w_u}{m_{11}};\ \delta_v = \frac{m_{33}w_v - m_{23}w_r}{m_{22}m_{33} - m_{23}m_{32}};\ \delta_r = \frac{-m_{32}w_v + m_{22}w_r}{m_{22}m_{33} - m_{23}m_{32}}.$$

From equation (2), we observe that for an underactuated ASV, the sway (lateral) motion and yaw motion are constrained. It is not possible to control yaw and sway independently at the same time. Moreover, in practice, the control point of an ASV is often centered at the center of gravity. As a result, $b_v \ll b_r$ (if the added mass in the dynamic model of ASV is neglected, then $b_v = 0$). This implies that the moment has a significant influence on the change in heading angle and little impact on sway motion. In other words, controlling lateral motion becomes more difficult because the control component $b_v T$ is small. To address this issue, a new control hand-point (H) different from the center of gravity (G) is selected, which lies on the longitudinal axis of the ASV (x_b axis) at distance L from the center of gravity (figure 1). In this case, the dynamic model of the ASV changes in a way that increases the control component in the sway direction. Indeed:

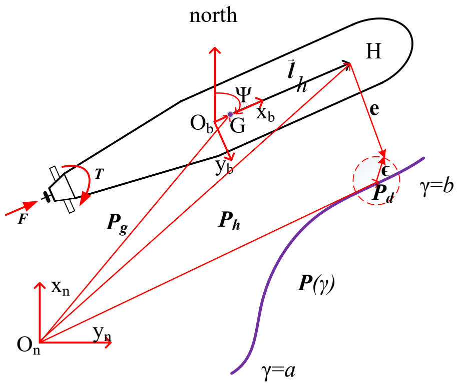

***Figure 1.** ASV in path-following with a new control handpoint H.*

According to [11], for a new control hand-point:

$$\boldsymbol{\upsilon}_h = \begin{bmatrix} u_h \\ v_h \end{bmatrix} = \begin{bmatrix} u \\ v + Lr \end{bmatrix} \tag{3}$$

$$\dot{\boldsymbol{\upsilon}}_h = \begin{bmatrix} \dot{u}_h \\ \dot{v}_h \end{bmatrix} = \begin{bmatrix} (f_u - Lr^2) + b_u F + \delta_u \\ (f_v + Lf_r) + (b_v + Lb_r)T + (\delta_v + L\delta_r) \end{bmatrix} = \boldsymbol{f}_h + \boldsymbol{u}_h + \boldsymbol{\delta}_h \tag{4}$$

Where:

$$\boldsymbol{f}_h = \begin{bmatrix} f_u - Lr^2 \\ f_v + Lf_r \end{bmatrix};\ \boldsymbol{u}_h = \begin{bmatrix} b_u F \\ (b_v + Lb_r)T \end{bmatrix};\ \boldsymbol{\delta}_h = \begin{bmatrix} \delta_u \\ \delta_v + L\delta_r \end{bmatrix} \tag{5}$$

It can be seen that the sway control component in equation (4) increases to $(b_v + Lb_r)T$ compared to $b_v T$ in (2).

2.2. Loose path-following with a small error

Let a path be given by parametric equation: $\boldsymbol{P}_d(\gamma)=\left[x_d(\gamma), y_d(\gamma)\right]^T$, where γ path parameter $\gamma\in\left[a,b\right]$. In the strict tracking problem:

$$\begin{cases} \boldsymbol{e}(\gamma(t))\to 0 \\ \boldsymbol{\upsilon}_h(\gamma(t))\to\boldsymbol{\upsilon}_d \end{cases}, t\to\infty \tag{6}$$

Where, $\boldsymbol{e}\triangleq\boldsymbol{P}_d(\gamma)-\boldsymbol{P}_h$ is the cross tracking error; $\boldsymbol{\upsilon}_d=\boldsymbol{P}'_d\dot{\gamma}$. In the body frame $\boldsymbol{e}^b\triangleq\boldsymbol{R}^T(\psi)\boldsymbol{e}=\boldsymbol{R}^T(\psi)(\boldsymbol{P}_d(\gamma)-\boldsymbol{P}_h)$.

In the loose tracking problem, a small error $\boldsymbol{\varepsilon}=\left[\varepsilon_1 \quad \varepsilon_2\right]^T$ is added to the discrepancy between the ASV's actual and desired positions. This implies that it is sufficient to drive the ASV to within an ε-neighborhood of the desired position ($\boldsymbol{P}_d$):

$$\boldsymbol{e}^b\triangleq\boldsymbol{R}^T(\psi)(\boldsymbol{P}_d(\gamma)-\boldsymbol{P}_h)+\boldsymbol{\varepsilon} \tag{7}$$

The time derivative of equation (7) is taken as follows:

$$\dot{\boldsymbol{e}}^b=-\boldsymbol{S}(r)\boldsymbol{e}^b+\boldsymbol{S}(r)\boldsymbol{\varepsilon}-\boldsymbol{\upsilon}_h^b+\boldsymbol{R}^T(\psi)\boldsymbol{P}'_d(\gamma)\dot{\gamma} \tag{8}$$

Design a loose tracking guidance law as follows:

$$\boldsymbol{\upsilon}_{ref}^b=k_p\boldsymbol{e}^b+\boldsymbol{R}^T(\psi)\boldsymbol{P}'_d(\gamma)\dot{\gamma}_d+\boldsymbol{S}(r)\boldsymbol{\varepsilon} \tag{9}$$

$$\ddot{\gamma}=-k_\gamma e_\gamma+\ddot{\gamma}_d-(\boldsymbol{e}^b)^T\boldsymbol{R}^T(\psi)\boldsymbol{P}'_d(\gamma) \tag{10}$$

Where: $\boldsymbol{R}(\psi)=\begin{bmatrix}\cos(\psi) & -\sin(\psi)\\ \sin(\psi) & \cos(\psi)\end{bmatrix}$ is the rotation matrix from the body frame to the navigation frame; $\dot{\gamma}_d\triangleq U_d/\|\boldsymbol{P}'_d\|$; $\boldsymbol{S}(r)=\begin{bmatrix}0 & -r\\ r & 0\end{bmatrix}$; $k_\gamma>0; k_p>0$; $U_d=\|\boldsymbol{\upsilon}_d\|$ is the desired speed of ASV.

Theorem 1**:** Assuming that $P(\gamma)$ is twice continuously differentiable with respect to the path parameter. Under the guidance law defined by (9) and under the assumption that $\boldsymbol{\upsilon}_h^b=\boldsymbol{\upsilon}_{h,ref}^b$, the ASV asymptotically converges to the desired path with a small position error $\|\boldsymbol{\varepsilon}\|$.

Proof. Consider the Lyapunov function:

$V_1=\frac{1}{2}\boldsymbol{x}^T\boldsymbol{x}$ với $\boldsymbol{x}\triangleq\left[(\boldsymbol{e}^b)^T, e_\gamma\right]^T$. It is clear that $V_1>0, \forall\boldsymbol{x}\neq 0, V_1(\boldsymbol{0})=0$. Take the derivative of V_1 with respect to time:

$$\dot{V}_1=\frac{1}{2}(\dot{\boldsymbol{x}}^T\boldsymbol{x}+\boldsymbol{x}^T\dot{\boldsymbol{x}})=\boldsymbol{x}^T\dot{\boldsymbol{x}}=\left[(\boldsymbol{e}^b)^T, e_\gamma\right]\left[(\dot{\boldsymbol{e}}^b)^T, \dot{e}_\gamma\right]^T=(\boldsymbol{e}^b)^T\dot{\boldsymbol{e}}^b+e_\gamma\dot{e}_\gamma \tag{11}$$

Where:

$$e_\gamma\triangleq\dot{\gamma}-\dot{\gamma}_d=\dot{\gamma}-\frac{U_d}{\|\boldsymbol{P}'_d\|}; \dot{e}_\gamma\triangleq\ddot{\gamma}-\ddot{\gamma}_d \tag{12}$$

Substitute $e_\gamma, \dot{e}_\gamma$ from (12), $\dot{\boldsymbol{e}}^b$ from (8) and $\boldsymbol{\upsilon}_h^b=\boldsymbol{\upsilon}_{h,ref}^b$ into (11). Then, we have:

$$\begin{aligned}\dot{V}_1 &= (\boldsymbol{e}^b)^T(-\boldsymbol{S}(r)\boldsymbol{e}^b + \boldsymbol{S}(r)\boldsymbol{\varepsilon} - \boldsymbol{\upsilon}_h^b + \boldsymbol{R}^T\boldsymbol{P}_d'\dot{\gamma}) + e_\gamma(\ddot{\gamma} - \ddot{\gamma}_d) \\ &= -(\boldsymbol{e}^b)^T\boldsymbol{S}(r)\boldsymbol{e}^b + (\boldsymbol{e}^b)^T(\boldsymbol{S}(r)\boldsymbol{\varepsilon} - \boldsymbol{\upsilon}_{h,ref}^b + \boldsymbol{R}^T\boldsymbol{P}_d'\dot{\gamma}) + e_\gamma(-k_\gamma e_\gamma - (\boldsymbol{e}^b)^T\boldsymbol{R}^T\boldsymbol{P}_d') \\ &= (\boldsymbol{e}^b)^T(\boldsymbol{S}(r)\boldsymbol{\varepsilon} - k_p\boldsymbol{e}^b - \boldsymbol{R}^T\boldsymbol{P}_d'\dot{\gamma}_d - \boldsymbol{S}(r)\boldsymbol{\varepsilon} + \boldsymbol{R}^T\boldsymbol{P}_d'\dot{\gamma}) - k_\gamma e_\gamma^2 - e_\gamma(\boldsymbol{e}^b)^T\boldsymbol{R}^T\boldsymbol{P}_d' \\ &= -k_p(\boldsymbol{e}^b)^T\boldsymbol{e}^b + (\boldsymbol{e}^b)^T(\dot{\gamma} - \dot{\gamma}_d)\boldsymbol{R}^T\boldsymbol{P}_d' - k_\gamma e_\gamma^2 - e_\gamma(\boldsymbol{e}^b)^T\boldsymbol{R}^T\boldsymbol{P}_d' \\ &= -k_p(\boldsymbol{e}^b)^T\boldsymbol{e}^b - k_\gamma e_\gamma^2 \le -\min\{k_p, k_\gamma\}\|\boldsymbol{x}\|^2 \le 0\end{aligned} \tag{13}$$

Here, we note that $(\boldsymbol{e}^b)^T\boldsymbol{S}(r)\boldsymbol{e}^b = 0, \forall \boldsymbol{e}^b$. From (13) it is inferred that V_1 decreases. In addition, V_1 is bonded below by 0, then $\lim_{t\to\infty} V_1(t)$ exist and is uniformly bonded. Then $\lim_{t\to\infty}\int_0^t V_1 d\tau = \lim_{t\to\infty} V_1(t) - V_1(0)$ exists and is uniformly bounded. According to Barbălat's lemma: $\lim_{t\to\infty} V_1 = 0$. Hence $\|\boldsymbol{x}\| \to 0$ as $t \to \infty$. As a result: $\boldsymbol{e}^b \to 0, e_\gamma \to 0$. This means that $\|\boldsymbol{P}_d'(\gamma) - \boldsymbol{P}_h\| \to \|\boldsymbol{\varepsilon}\|$.

2.3. Design a robust adaptive controller

We define a sliding parameter as follows:

$$\boldsymbol{s}^b = \boldsymbol{\upsilon}_h^b - \boldsymbol{\upsilon}_{ref}^b \tag{14}$$

Taking the derivative of equation (14) and combining it with (8), we obtain:

$$\begin{aligned}\dot{\boldsymbol{s}}^b &= \dot{\boldsymbol{\upsilon}}_h^b - \dot{\boldsymbol{\upsilon}}_{ref}^b = \boldsymbol{f}_h + \boldsymbol{\delta}_h + \boldsymbol{u}_h - \frac{d}{dt}(k_p\boldsymbol{e}^b + \boldsymbol{R}^T\boldsymbol{P}_d'\dot{\gamma}_d + \boldsymbol{S}(r)\boldsymbol{\varepsilon}) \\ &= \boldsymbol{f}_h + \boldsymbol{\delta}_h + \boldsymbol{u}_h - k_p\dot{\boldsymbol{e}}^b - \dot{\boldsymbol{R}}^T\boldsymbol{P}_d'\dot{\gamma}_d - \boldsymbol{R}^T(\boldsymbol{P}_d''\dot{\gamma}\dot{\gamma}_d + \boldsymbol{P}_d'\ddot{\gamma}_d) - \boldsymbol{S}(1)\boldsymbol{\varepsilon}\dot{r}) \\ &= \boldsymbol{f}_h + \boldsymbol{\delta}_h + \boldsymbol{u}_h - k_p\dot{\boldsymbol{e}}^b - \boldsymbol{S}(1)\boldsymbol{\varepsilon}(f_r + \delta_r + b_rT) + \boldsymbol{S}(r)\boldsymbol{R}^T\boldsymbol{P}_d'\dot{\gamma}_d - \boldsymbol{R}^T(\boldsymbol{P}_d''\dot{\gamma}\dot{\gamma}_d + \boldsymbol{P}_d'\ddot{\gamma}_d) \\ &= \boldsymbol{f}_h - \boldsymbol{S}(1)\boldsymbol{\varepsilon}f_r + (\boldsymbol{\delta}_h - \boldsymbol{S}(1)\boldsymbol{\varepsilon}\delta_r) + \begin{bmatrix} b_u & \varepsilon_2 b_r \\ 0 & b_v + Lb_r - \varepsilon_1 b_r\end{bmatrix}\begin{bmatrix} F \\ T\end{bmatrix} - k_p\dot{\boldsymbol{e}}^b + \boldsymbol{S}(r)\boldsymbol{R}^T\boldsymbol{P}_d'\dot{\gamma}_d \\ &\quad - \boldsymbol{R}^T(\boldsymbol{P}_d''\dot{\gamma}\dot{\gamma}_d + \boldsymbol{P}_d'\ddot{\gamma}_d)\end{aligned} \tag{15}$$

Let $\boldsymbol{B}_u = \begin{bmatrix} b_u & \varepsilon_2 b_r \\ 0 & b_v + Lb_r - \varepsilon_1 b_r\end{bmatrix}$. This matrix is invertible if $b_v + Lb_r - \varepsilon_1 b_r \ne 0$.

Let $\boldsymbol{x} \triangleq \begin{bmatrix}(\boldsymbol{e}^b)^T & e_\gamma\end{bmatrix}^T$ and choose an adaptive parameter:

$$\dot{\hat{\beta}} = k_\beta\|\boldsymbol{s}^b\|_1, \text{ with } \hat{\beta}(0) > 0, k_\beta > 0 \tag{16}$$

A robust adaptive force controller is designed as follows:

$$\begin{bmatrix} F \\ T\end{bmatrix} = \boldsymbol{B}_u^{-1}\left(-k_s\boldsymbol{s}^b - \boldsymbol{f}_h + \boldsymbol{S}(1)\boldsymbol{\varepsilon}f_r - \hat{\beta}sign(\boldsymbol{s}^b) + k_p\dot{\boldsymbol{e}}^b - \boldsymbol{S}(r)\boldsymbol{R}^T\boldsymbol{P}_d'\dot{\gamma}_d + \boldsymbol{R}^T(\boldsymbol{P}_d''\dot{\gamma}\dot{\gamma}_d + \boldsymbol{P}_d'\ddot{\gamma}_d)\right) \tag{17}$$

Theorem 2: Consider the dynamics of the ASV given by equation (2), with the reference velocity and path parameter defined by the guidance laws (9) and (10), respectively. Suppose that the path is twice differentiable with respect to the path parameter γ. Then, under the adaptive controller defined by (17), and the condition $4k_sk_P > 1$, the ASV asymptotically converges to the desired path with a small position error as time tends to infinity.

Proof**:** Consider the Lyapunov function:

$$V_2 = V_1 + \frac{1}{2}\left\| \boldsymbol{s}^b \right\|^2 + \frac{1}{2k_\beta}(\hat{\beta} - \bar{\beta})^2 = \frac{1}{2}\left\| (\boldsymbol{e}^b)^T, \quad e_\gamma \right\|^2 + \frac{1}{2}\left\| \boldsymbol{s}^b \right\|^2 + \frac{1}{2k_\beta}(\hat{\beta} - \bar{\beta})^2 \tag{18}$$

Here, the constant $\bar{\beta}$ can be selected large enough to ensure that $\left\| \boldsymbol{\delta}_h - \boldsymbol{S}(1)\boldsymbol{\varepsilon}\delta_r \right\|_\infty < \bar{\beta}$.

Since F and T in (17) are discontinuous inputs, the stability of the closed-loop system can be analyzed in the sense of Filippov [14].

Take the derivative of equation (17):

$$\dot{V}_2 = (\boldsymbol{e}^b)^T \dot{\boldsymbol{e}}^b + e_\gamma \dot{e}_\gamma + (\boldsymbol{s}^b)^T \dot{\boldsymbol{s}}^b + (\hat{\beta} - \bar{\beta})\left\| \boldsymbol{s}^b \right\|_1 \tag{19}$$

Substitute $\boldsymbol{e}^b$ from (8), $\dot{e}_\gamma$ from (12), $\dot{\boldsymbol{s}}^b$ from (15), $\boldsymbol{\upsilon}_h^b$ from (14) and $\begin{bmatrix} F \\ T \end{bmatrix}$ from (17) into (19). Then we obtain:

$$\begin{aligned}
\dot{V}_2 &= (\boldsymbol{e}^b)^T \left[-\boldsymbol{S}(r)\boldsymbol{e}^b + \boldsymbol{S}(r)\boldsymbol{\varepsilon} - \boldsymbol{\upsilon}_h^b + \boldsymbol{R}^T \boldsymbol{P}_d' \dot{\gamma} \right] + e_\gamma \left[-k_\gamma e_\gamma - (\boldsymbol{e}^b)^T \boldsymbol{R}^T \boldsymbol{P}_d' \right] \\
&+ (\boldsymbol{s}^b)^T \left[-k_s \boldsymbol{s}^b - \hat{\beta} sign(\boldsymbol{s}^b) + (\boldsymbol{\delta}_h - \boldsymbol{S}(1)\boldsymbol{\varepsilon}\delta_r) \right] + (\hat{\beta} - \bar{\beta})\left\| \boldsymbol{s}^b \right\|_1 \\
&= (\boldsymbol{e}^b)^T \left[\boldsymbol{S}(r)\boldsymbol{\varepsilon} - \boldsymbol{s}^b - \boldsymbol{\upsilon}_{ref}^b + \boldsymbol{R}^T \boldsymbol{P}_d' \dot{\gamma} \right] - k_\gamma e_\gamma^2 - (\boldsymbol{e}^b)^T \boldsymbol{R}^T \boldsymbol{P}_d' e_\gamma - k_s \left\| \boldsymbol{s}^b \right\|^2 \\
&- \hat{\beta}\left\| \boldsymbol{s}^b \right\|_1 + (\boldsymbol{s}^b)^T (\boldsymbol{\delta}_h - \boldsymbol{S}(1)\boldsymbol{\varepsilon}\delta_r) + (\hat{\beta} - \bar{\beta})\left\| \boldsymbol{s}^b \right\|_1 \\
&\le (\boldsymbol{e}^b)^T (-\boldsymbol{s}^b - k_p \boldsymbol{e}^b + \boldsymbol{R}^T \boldsymbol{P}_d' e_\gamma) - k_\gamma e_\gamma^2 - (\boldsymbol{e}^b)^T \boldsymbol{R}^T \boldsymbol{P}_d' e_\gamma - k_s \left\| \boldsymbol{s}^b \right\|^2 \\
&- \hat{\beta}\left\| \boldsymbol{s}^b \right\|_1 + (\boldsymbol{s}^b)^T (\boldsymbol{\delta}_h - \boldsymbol{S}(1)\boldsymbol{\varepsilon}\delta_r) + (\hat{\beta} - \bar{\beta})\left\| \boldsymbol{s}^b \right\|_1 \\
&\le (\boldsymbol{e}^b)^T (-\boldsymbol{s}^b - k_p \boldsymbol{e}^b + \boldsymbol{R}^T \boldsymbol{P}_d' e_\gamma) - k_\gamma e_\gamma^2 - (\boldsymbol{e}^b)^T \boldsymbol{R}^T \boldsymbol{P}_d' e_\gamma - k_s \left\| \boldsymbol{s}^b \right\|^2 \\
&+ \left\| (\boldsymbol{s}^b)^T \right\|_1 \left\| \boldsymbol{\delta}_h - \boldsymbol{S}(1)\boldsymbol{\varepsilon}\delta_r \right\|_\infty - \bar{\beta})\left\| \boldsymbol{s}^b \right\|_1 \\
&\le -k_p \left\| \boldsymbol{e}^b \right\|^2 - (\boldsymbol{e}^b)^T \boldsymbol{s}^b - k_\gamma e_\gamma^2 - k_s \left\| \boldsymbol{s}^b \right\|^2 - (\bar{\beta} - \left\| \boldsymbol{\delta}_h - \boldsymbol{S}(1)\boldsymbol{\varepsilon}\delta_r \right\|_\infty)\left\| \boldsymbol{s}^b \right\|_1 \\
&\le -k_p \left\| \boldsymbol{e}^b + \frac{\boldsymbol{s}^b}{2k_p} \right\|^2 - (k_s - \frac{1}{4k_p})\left\| \boldsymbol{s}^b \right\|^2 - k_\gamma e_\gamma^2 \le 0
\end{aligned} \tag{20}$$

Here, we use the condition $4k_s k_P > 1$ and note that $(\boldsymbol{e}^b)^T \boldsymbol{S}(r)\boldsymbol{e}^b = 0, \forall \boldsymbol{e}^b$. From equation (20), we infer that V_2 decreases. In addition, since V_2 is bounded below by 0, then V_2 is uniformly bounded. As a result, $\boldsymbol{e}^b, e_\gamma, \boldsymbol{s}^b, \hat{\beta}$ are uniformly bounded $(\in L_\infty)$. Then $\boldsymbol{\upsilon}^b$ uniformly bounded. According to LaSalle–Yoshizawa's lemma, it follows that $\lim_{t\to\infty}\left(k_p \left\| \boldsymbol{e}^b + \frac{\boldsymbol{s}^b}{2k_p} \right\| + (k_s - \frac{1}{4k_p})\left\| \boldsymbol{s}^b \right\|^2 + k_\gamma e_\gamma^2 \right) = 0$. Then: $\boldsymbol{e}^b + \frac{\boldsymbol{s}^b}{2k_\gamma} \to 0, \boldsymbol{s}^b \to 0, e_\gamma \to 0$. As a result, $\boldsymbol{e}^b \to 0$, which means that the ASV converges to the desired path with a small error $\left\| \boldsymbol{\varepsilon} \right\|$.

Note**:** Unlike the SMC controller, the controller in equation (17) does not require knowledge of the upper bound of the disturbance. Instead, it uses an adaptive parameter with an initial value $\hat{\beta}(0)$.

3. SIMULATION AND DISCUSSION

The simulation is performed with a circular path using the MATLAB Simulink tool. The path is defined as:

$\begin{cases} \boldsymbol{P}_d(t) = [100\cos(0.5t) \quad 100\sin(0.5t)]^T \\ \quad t \in (0 \quad 150) \end{cases}$. The initial conditions at $t = 0$ are : $\boldsymbol{P}_d(0) = [90 \quad 5]^T$, $\psi(0) = \frac{\pi}{3}$, $u(0) = 0$, $v(0) = 0$, $r(0) = 0$; the desired velocity $U_d = 0.6$ (m/s), $k_p = 0.5$, $k_s = 0.52$, $k_\beta = 0.05$, $k_\gamma = 0.52$, $\gamma(0) = 0$, $\dot{\gamma}(0) = 0$. The parameters of the ASV model are specified in table 1.

Table 1. *The parameters of the ASV model.*

m_{11}	200 kg	d_{11}	70 kg/s	c_1	200 kg/rad
m_{22}	200 kg	d_{22}	100 kg/s	c_2	200 kg/rad
$m_{23} = m_{32}$	20 kg.m	$d_{23} = d_{32}$	-30 kg.m/s	c_3	20 kg/rad^2
m_{33}	700 kg.m^2	d_{33}	50 kg.m^2/s	L	1 m

Here, $m_{11} = m_{22} = m$ is the mass of the ASV; m_{33} is the moment of inertia about the yaw axis through the center of mass; m_{23} is the coefficient representing the effect of angular acceleration on sway velocity; m_{32} is the coefficient representing the effect of sway acceleration on angular velocity; d_{11}, d_{22},.. are damping coefficients; c_1, c_2, c_3 are Coriolis–centripetal coefficients; and L is the distance from the control hand-point to the center of mass of ASV.

The model is subjected to disturbances with an amplitude approximately equal to 25% of the ASV's mass.

With $\boldsymbol{\varepsilon} = \boldsymbol{e}_1 = [0.4 \quad 0.3]^T$ and L = 1 m, the simulation results are shown in figures 2 - 7.

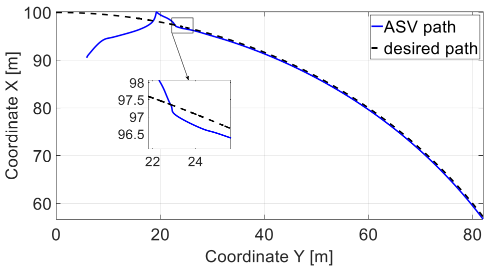

Figure 2. *ASV path under controller (17).*

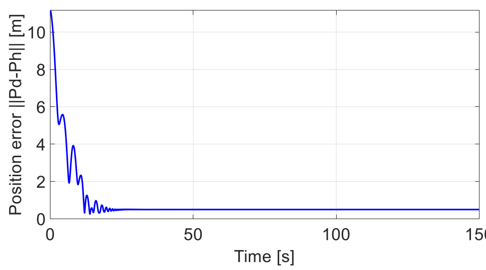

Figure 3. *Position error vs time.*

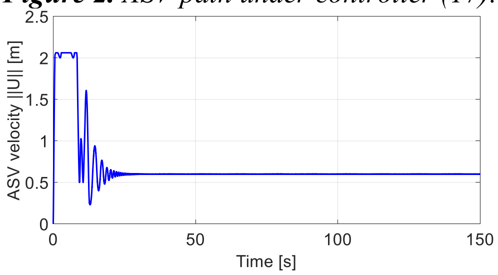

Figure 4. *ASV velocity vs time.*

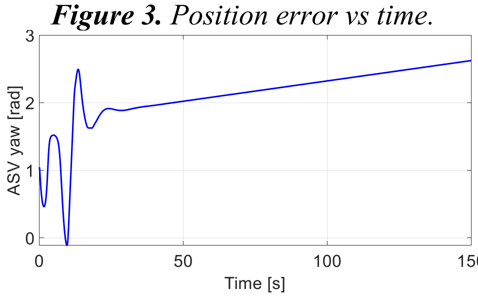

Figure 5. *ASV yaw angle vs time.*

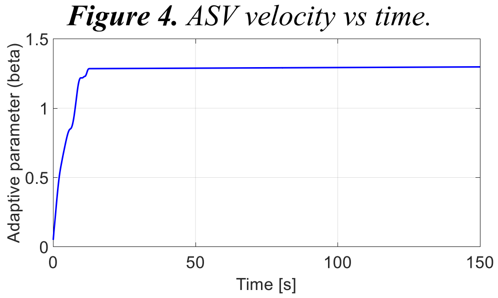

Figure 6. *Adaptive parameter vs time.*

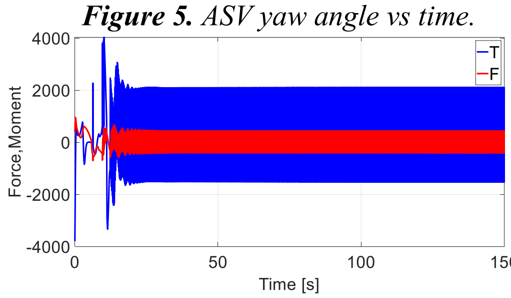

Figure 7. *Control force and moment.*

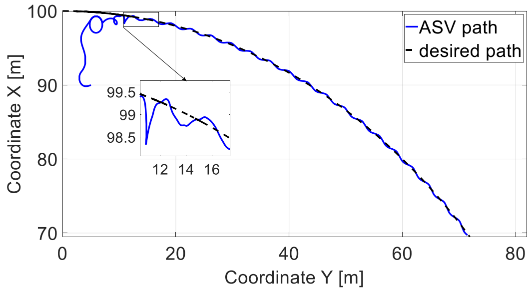

Figure 8. *ASV path with L = 0 m.*

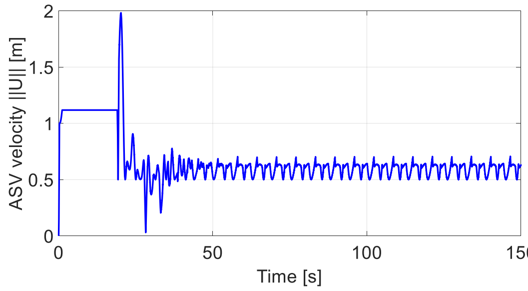

Figure 9. *ASV velocity with L = 0 m.*

It can be seen that the ASV tracks the desired trajectory with a position error that asymptotically approaches the added error $\|\boldsymbol{\varepsilon}\|$: $\|\boldsymbol{P}_d - \boldsymbol{P}_h\| \to \|\boldsymbol{e}_1\| = 0.5$ (figures 2 and 3). The ASV's velocity tracks the desired velocity $U_d = 0.6$(m/s) with an arbitrary error bounded by $|r|\|\boldsymbol{e}\|$(figure 4). The adaptive parameter increases rapidly during the setting phase and then continues to increase steadily toward its limit during the tracking phase (figure 6). The ASV heading, fluctuating in the setting phase, gradually increases as it follows the circular trajectory (figure 5). Due to the effect of the sign function in the force control law, the control force and moment exhibit oscillations (figure 7).

In comparison to the case where the new control hand-point is not applied (L= 0 m), the ASV's path and velocity show greater fluctuations (figures 8 and 9).

Figure 10 compares ASV trajectories with different added errors ($\boldsymbol{\varepsilon} = \boldsymbol{e}_2 = [0.5 \quad 0]^T$, $\boldsymbol{\varepsilon} = \boldsymbol{e}_3 = [0 \quad 0.5]^T$, $\boldsymbol{\varepsilon} = \boldsymbol{e}_4 = [0 \quad -0.5]^T$). In all cases, the ASV follows the desired trajectory with a position error approaching $\|\boldsymbol{\varepsilon}\|$. Additionally, depending on the value of ε_2, the ASV trajectory may lie to the left ($\varepsilon_2 < 0$), to the right $\varepsilon_2 > 0$ or coincide with the desired trajectory but be shifted along the axis x_b with a value of ε_1.

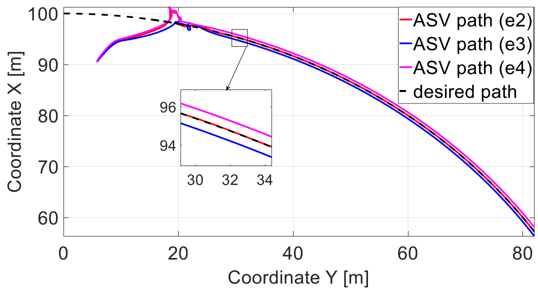

Figure 10. *Comparison of ASV path with different added errors (e₂, e₃, e₄).*

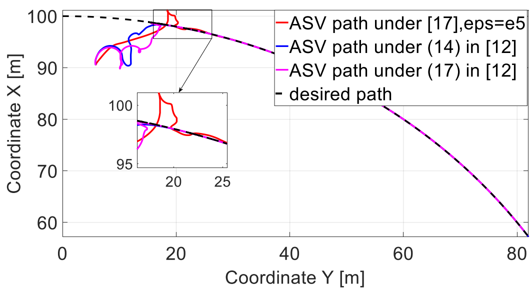

Figure 11. *Compare the ASV path under the proposed controller with $\|\boldsymbol{\varepsilon}\| = 0$ and under (14), (17) in [12].*

In the case of $\boldsymbol{\varepsilon} = \boldsymbol{e}_5 = [0 \quad 0]^T$, the loose tracking problem becomes a strict tracking problem. Figure 11 compares the ASV paths under the proposed control law with $\boldsymbol{\varepsilon} = \boldsymbol{e}_5 = [0 \quad 0]^T$ and under the controllers (14), (17) from [12] for the strict tracking problem. With the three controllers, the tracking quality is quite similar; the ASV follows the desired path asymptotically. In the cases of loose tracking with $\|\boldsymbol{\varepsilon}\| = 0$ and tight tracking according to (14) and (17) from [12], it can be observed that the loose tracking controller has a later tracking start point than the other two controllers. However, the loose tracking controller is more general, allowing adjustment of the relative position between the ASV trajectory and the desired trajectory. This can be particularly useful in scenarios where the ASV is towed by another vehicle, and it is necessary to maintain a fixed relative distance between the leading vehicle and the ASV.

4. CONCLUSIONS

The paper proposes a robust adaptive controller for ASV path-following based on the idea of adding a small error to the tracking error. A guidance law is designed to ensure that ASV will track the desired path with a small error when the ASV velocity tracks the reference velocity given by the guidance law. A robust force control law with an adaptive parameter is also developed to ensure that the ASV's velocity tracks the reference velocity despite unknown disturbances. Simulation results show that, with the proposed controller, the ASV asymptotically converges to the desired path with an arbitrary small error. The simulations also demonstrate that the ASV achieves better tracking performance when using the proposed control hand-point, compared to the case where the hand-point is not adjusted (L=0 m). In the case $\|\boldsymbol{\varepsilon}\| = 0$, the loose tracking problem becomes a strict tracking problem, and the proposed controller exhibits performance comparable to controllers (14) and (17) in [12].

Acknowledgement: *The author would like to sincerely thank Dr. Tran Van Quoc, School of Mechanical Engineering, Hanoi University of Science and Technology, for his valuable support in completing this article.*

REFERENCES

[1]. TI Fossen, *"An adaptive line-of-sight (ALOS) guidance law for path following of aircraft and marine craft",* IEEE Transactions on Control Systems Technology, Vol.31, Iss.6, (2023).

[2]. Børhaug E, Pavlov A, Pettersen KY, *"Integral LOS control for path following of underactuated marine surface vessels in the presence of constant ocean currents"*. In: 47th IEEE Conference on Decision and Control, 4984-4991, (2008).

[3]. Yamasaki T, Enomoto K, Takano H, Baba Y, Balakrishnan SN, *"Advanced pure pursuit guidance via sliding mode approach for chase UAV"*. AIAA Guid. Navig. Control Conf. Exhib, (2009).

[4]. Xu, H. T., and C. Guedes Soares. *"Waypoint-following for a marine surface ship model based on vector field guidance law."* Maritime Technology and Engineering 3: 409-418, (2016).

[5]. Kobatake, Kanako, Tadatsugi Okazaki, and Masakazu Arima. *"Study on optimal tuning of pid autopilot for autonomous surface vehicle."* Ifac-PapersOnLine 52.21: 335-340, (2019).

[6]. Elmokadem, Taha, Mohamed Zribi, and Kamal Youcef-Toumi. *"Trajectory tracking sliding mode control of underactuated AUVs."* Nonlinear Dynamics 84: 1079-1091, (2016).

[7]. Su Y., Wan L., Zhang D., and Huang F., *"An improved adaptive integral line-of-sight guidance law for unmanned surface vehicles with uncertainties"*, Appl. Ocean Res. 108, (2021).

[8]. C. Lee, Q. Van Tran, J. Kim, *"Safety-guaranteed ship berthing using cascade tubebased model predictive control"*. IEEE Trans. Control Syst. Technol., 32(4), pp.1504–1511, (2024).

[9]. Liu, Cheng, Ting Sun, and Xuegang Wang. *"Constrained LOS guidance for path following of underactuated marine vehicle with input saturation."* Ocean Engineering 307, (2024).

[10]. A. P. Aguiar, J. A. P. Hespanha, *"Trajectory-tracking and path-following of underactuated autonomous vehicles with parametric modeling uncertainty"*. IEEE Transactions on Automatic Control, 52(8), pp. 1362–1379, (2007).

[11]. Cao Duc Sang et. al., *"Điều khiển di chuyển bám quỹ đạo cho phương tiện nổi tự hành hụt dẫn động dựa trên kỹ thuật mô hình dự báo phi tuyến"*, Journal of Science and Technology, Hanoi University of Industry, Vol. 61, No. 3, (2025) (in Vietnamese).

[12]. Duc Sang Cao, Quoc Van Tran, *"Adaptive path-following control of underactuated surface vessels subject to unknown disturbances with uniform bounded lateral motion"*, International Journal of Control, Automation, and Systems, Vol. 23, (2025).

[13]. Fossen T. I., *"Handbook of Marine Craft Hydrodynamics and Motion Control"*, Wiley, (2011).

TÓM TẮT

Thiết kế bộ điều khiển bền vững thích nghi cho ASV hụt dẫn động trong bài toán bám lỏng dựa trên kỹ thuật bổ sung sai số vị trí và lựa chọn điểm điều khiển mới

Điều khiển ASV di chuyển bám quỹ đạo là một thách thức không nhỏ do môi trường ASV hoạt động có cấu trúc thiếu ổn định và thường xuyên chịu ảnh hưởng của nhiễu như gió, sóng biển, dòng hải lưu. Thêm vào đó, mô hình động lực của ASV có độ phi tuyến cao và chứa nhiều yếu tố bất định. Trong công trình này, tác giả xây dựng một bộ điều khiển thích nghi cho bài toán điều khiển ASV bám quỹ đạo trong điều kiện nhiễu bất định. Để giải quyết vấn đề hụt dẫn động, một sai số nhỏ được bổ sung vào sai số bám vị trí, đồng thời áp dụng kỹ thuật thay đổi điểm điều khiển. Các luật dẫn và luật điều khiển cho phần lực được thiết kế và chứng minh tính ổn định dựa trên lý thuyết ổn định Lyapunov. Ngoài chứng minh tính ổn định, các kết quả mô phỏng trên bộ công cụ Matlab-Simulink khẳng định tính đúng đắn của bộ điều khiển đề xuất. Các kết quả mô phỏng cũng so sánh với trường hợp không thay đổi điểm điều khiển và so sánh với bộ điều khiển bám chặt và bộ điều khiển bám lỏng khi sai số bổ sung chọn bằng 0.

Từ khoá: ASV hụt dẫn động; Sai số bám; Điểm điều khiển; Di chuyển bám quỹ đạo.